

Award Number: DAMD17-03-1-0743

TITLE: Acoustic Emission Based Surveillance System for Prediction of Stress Fractures

PRINCIPAL INVESTIGATOR: Ozan Akkus, Ph.D.

CONTRACTING ORGANIZATION: The University of Toledo, Toledo, OH 43606-3390

REPORT DATE: September 2006

TYPE OF REPORT: Annual

PREPARED FOR: U.S. Army Medical Research and Materiel Command

Fort Detrick, Maryland 21702-5012

DISTRIBUTION STATEMENT: Approved for Public Release;

Distribution Unlimited

The views, opinions and/or findings contained in this report are those of the author(s) and should not be construed as an official Department of the Army position, policy or decision unless so designated by other documentation.

REPORT DOCUMENTATION PAGE				Form Approved OMB No. 0704-0188	
Public reporting burden for this collection of information is estimated to average 1 hour per response, including the time for reviewing instructions, searching existing data sources, gathering and maintaining the data needed, and completing and reviewing this collection of information. Send comments regarding this burden estimate or any other aspect of this collection of information, including suggestions for reducing this burden to Department of Defense, Washington Headquarters Services, Directorate for Information Operations and Reports (0704-0188), 1215 Jefferson Davis Highway, Suite 1204, Arlington, VA 22202-4302. Respondents should be aware that notwithstanding any other provision of law, no person shall be subject to any penalty for failing to comply with a collection of information if it does not display a currently valid OMB control number. PLEASE DO NOT RETURN YOUR FORM TO THE ABOVE ADDRESS.					
1. REPORT DATE September 2006		2. REPORT TYPE Annual		3. DATES COVERED 1 September 2005 - 31 August 2006	
4. TITLE AND SUBTITLE Acoustic Emission Based Surveillance System for Prediction of Stress Fractures				5a. CONTRACT NUMBER	
				5b. GRANT NUMBER DAMD17-03-1-0743	
				5c. PROGRAM ELEMENT NUMBER	
6. AUTHOR(S) Ozan Akkus				5d. PROJECT NUMBER	
				5e. TASK NUMBER	
				5f. WORK UNIT NUMBER	
7. PERFORMING ORGANIZATION NAME(S) AND ADDRESS(ES) The University of Toledo, Toledo, OH, 43606-3390				8. PERFORMING ORGANIZATION REPORT NUMBER	
9. SPONSORING / MONITORING AGENCY NAME(S) AND ADDRESS(ES) U.S. Army Medical Research and Materiel Command Fort Detrick, Maryland 21702-5012				10. SPONSOR/MONITOR'S ACRONYM(S)	
				11. SPONSOR/MONITOR'S REPORT NUMBER(S)	
12. DISTRIBUTION / AVAILABILITY STATEMENT Approved for Public Release; Distribution Unlimited					
13. SUPPLEMENTARY NOTES					
14. ABSTRACT Stress fractures of bone constitute the most serious musculoskeletal overuse injury during military training of male and female recruits. The hypothesis of our study is that the onset of stress fractures can be predicted by monitoring the evolution of microdamage activity using acoustic emissions. During the first year bone tissue was procured and amassed for specimen preparation. A sufficient number of donor tibias have been obtained and have been machined into test specimens. The test system was redesigned after the first year to improve the performance of both the mechanical testing as well as the acoustic emission detection of microdamage events. Different groups of beams will be tested to varying degrees of mechanical property degradation and relationship between the acoustic event parameters and fatigue failure will be studied. The third year activities focused on eliminating the artifactual emissions generated by sample motion over the loading supports which confound legitimate emissions from bone microcracking, and, characterization of the AE emission strength at the source and attenuation over time.					
15. SUBJECT TERMS					
16. SECURITY CLASSIFICATION OF:			17. LIMITATION OF ABSTRACT UU	18. NUMBER OF PAGES	19a. NAME OF RESPONSIBLE PERSON USAMRMC
a. REPORT U	b. ABSTRACT U	c. THIS PAGE U			19b. TELEPHONE NUMBER (include area code)

Table of Contents

Cover	(1)
SF 298	(2)
Introduction	(4)
Body	(4)
Key Research Accomplishments	(9)
Reportable outcomes	(9)
Conclusions	(9)

Introduction

Stress fracture involves generation and propagation of microfailure events in the cortical bone. Earlier studies examined damage accumulation during fatigue testing at different intervals using histology. Histology is useful to understand damage evolution; however, it is an inherently static process and it can reflect the temporal changes in microfailure processes only by time-consuming histological processing. Acoustic emission (AE, stress wave generated by microfailure events) may be able to predict the impending fatigue failure by simply monitoring the rate of accumulation of acoustic emission events. The overarching aim of this project is to develop a controlled fatigue loading model of cortical bone to investigate the acoustic emission events associated with microdamage formation. In the prior years of this project, human tibial bone was procured in an age range of about 20 to 50, including males and females. Standard beam-shaped bone specimens were prepared from these tibiae. We also focused on developing a mechanical loading fixture system that will minimize artifactual acoustic emissions from loading supports.

Body

Technical work conducted during this report period focused on: 1) refinement of interfering acoustic emission noise originating from loading supports, 2) measurement of the attenuation of acoustic emission waves in bone and other tissues, 3) measurement of acoustic emission amplitude associated with microcrack formation.

1) Refinement of interfering acoustic emission noise originating from loading supports,

Cadaveric human tibias from donors without any history of skeletal disease or trauma to the lower extremities were obtained from Musculoskeletal Transplant Foundation (MTF, Edison, NJ, USA). Tibia was chosen due to the common occurrence of stress fractures in tibia. Bone specimens were machined from the distal diaphysis of the tibias of 5 male and 5 female donors in an age range of 22 to 52. The distal segment of the diaphysis was further divided into three anatomical compartments (Fig. 1) using a low-speed metallurgical saw (Southbay Tech, CA, USA). Specimens of approximately 1.15 mm × 5.5 mm × 40mm in dimensions were machined in the longitudinal plane of tibia. Each specimen was polished serially with 600, 800, 1200 grits sandpapers and finally with the micro polishing papers with fine alumina powder (0.3 μm). Specimens were sonicated in distilled water with an ultrasonic cleaner (B200, Branson Ultrasonic Corporation, Danbury, CT) after each polishing step to eliminate loose particles generating noise during fatigue tests.

Fatigue loading was applied with a mechanical testing machine (800LE, Test Resources, Shakopee, MN). Load was measured with a 50 lb load-cell (Omega Engineering Inc., Stamford, CT) and actuator displacement was measured with a ± 0.5 mm range displacement gage (Epsilon Tech. Corp., Jackson, WY). Aluminum and Delrin were assessed as two types of candidate material for making the support blocks and the loading point (Fig. 1). As will be detailed later, aluminum supports induced wear on bone sample at contact points during fatigue and caused generation of acoustic noise. Delrin was used because of low friction coefficient and high dimensional stability. Both bottom supports and the loading tip were polished in the same way as the bone specimens, with 600, 800, 1200 grit sandpapers and micro polishing paper, followed by sonication.

Fatigue tests were performed under load control with a minimum to maximum load ratio of $R = 0.1$. An incremental loading regime in which the load was increased by 5% of the previous value was chosen to prevent catastrophic failures in the beginning of the test due to over-prescription of initial strain level while enabling fatigue failure in a reasonable time frame (less than a week). The maximum load corresponding to 0.85% initial strain was selected and applied to each sample for the first 2 hours. If the failure did not occur during the first two hours then the load was increased by 5% of the previous load to 0.893% strain for the next two hours. Beyond 4 hours of fatigue the load was kept at a level to generate an initial strain of 0.937% until failure. To find the load corresponding to the initial target strain level, samples were loaded between 1 N and 10 N for 50 cycles to calculate the initial stiffness (k_i) from the slope of the load vs. displacement

curve. Flexural modulus of the specimen (E_f) and load (P) corresponding to the desired initial strain level (ϵ) was calculated using beam bending equations.

Two AE sensors (R15- α , Physical Acoustics Corporation, NJ) were attached to the sides of the bottom supports with high viscosity vacuum grease for acoustic coupling (Fig. 1). Acoustic emission signals were amplified at 40 dB and filtered with a band-pass filter of 100-300 kHz (Physical Acoustics Corporation, NJ). AEs were continuously monitored with a two channel AMSY-5 data acquisition system (Vallen Systeme GmbH, Munich, Germany) at 2.5 MHz data acquisition rate per channel. AE monitoring settings were as follows: Rearm time of 1 ms, event discrimination time of 100 μ s. These values were selected based on the reverberation of pencil lead break generated emissions in the test set-up such that each pencil break were registered as one acoustic emission, eliminating reflections to be registered as additional events. AE threshold was increased to 42 dB during data processing conservatively to ensure the elimination of low level artifactual emissions. AE amplitude, the magnitude of the signal at the peak; duration, the time interval between the first and the last threshold crossing; rise time, the time interval from the first threshold crossing to the peak; number of counts, the number of pulses on the positive side of the spectrum; and AE energy, area of the triangle defined by amplitude, rise time and duration were recorded.

Source location was the main tool to identify noise coming from the outer-supports. Source location filter is based on the difference between the arrival times of an event at the two sensors. Since the specimen was loaded in the middle, equidistantly from both sensors, an AE emerging from the mid-point would trigger both sensors simultaneously, resulting in an arrival time difference (ΔT) of 0. If the source of event skews to either side from the mid-point then ΔT assumes a positive or negative value. The location of the source (x) then can be calculated by using ΔT , velocity of the wave (C) and the distance between the sensors (d), which is 61 mm in the setup. The mid-point is at $x = d/2$.

Event location parameters were tested/tuned for each specimen before the test by making 0.3 mm pencil lead breaks on the specimen. The mean ΔT for the pencil breaks in the middle of the specimen was 0.19 μ sec with a standard deviation of 2.4 μ sec. Therefore, emissions with ΔT values of less than 10 μ s corresponding approximately ± 12.5 mm vicinity of the mid-point were accepted as emissions sourcing from the middle of the sample. In three-point bending test, the span length was 30 mm. The 12.5 mm criterion is wide enough to cover the potential AE sources in the sample.

Samples tested with aluminum supports generated AEs in all three regions, indicating that there were compounding AEs due to friction and rubbing at the contact locations (Fig. 2A). Source location indicated that the emissions sourced from the entire length of the sample, with the most of the AEs originating from the middle section. When outer supports and loading tip material were changed to polished Delrin and the sample was secured at support blocks with orthodontic elastics the compounding noise coming from contacts were eliminated (Fig. 2B).

Table 1- Data Summary: Mean, median, minimum and maximum values of the key variables. Data excludes the two samples which released AEs just before the failure.

	Number of AEs	Modulus (GPa)	Fatigue Life (cycle)	Percent of fatigue life at the time of first AE event	Time to Failure after first AE (min)	Percent change in compliance at the first AE event
Mean	137	10.66	208522	95.35	62.4	18.1
Median	28	10.45	136469	98.17	16.9	17.4
Standard Deviation	375	1.81	200578	6.73	94	11.2
Min	6	8.57	20986	72.68	0.03	1.6
Max	1861	17.50	945054	99.99	370.4	45.6

The typical compliance curves obtained from three point bending fatigue tests displayed three regimes (Fig. 2). In the first region, compliance was increased linearly (Phase I in Fig. 2B) This region was followed by a nonlinear transition region (Phase II in Fig. 2B) where compliance was increased significantly, indicating the inception of damage processes in the specimen. In the last region, the increase in compliance became very rapid and concluded in failure (Phase III in Fig. 2B).

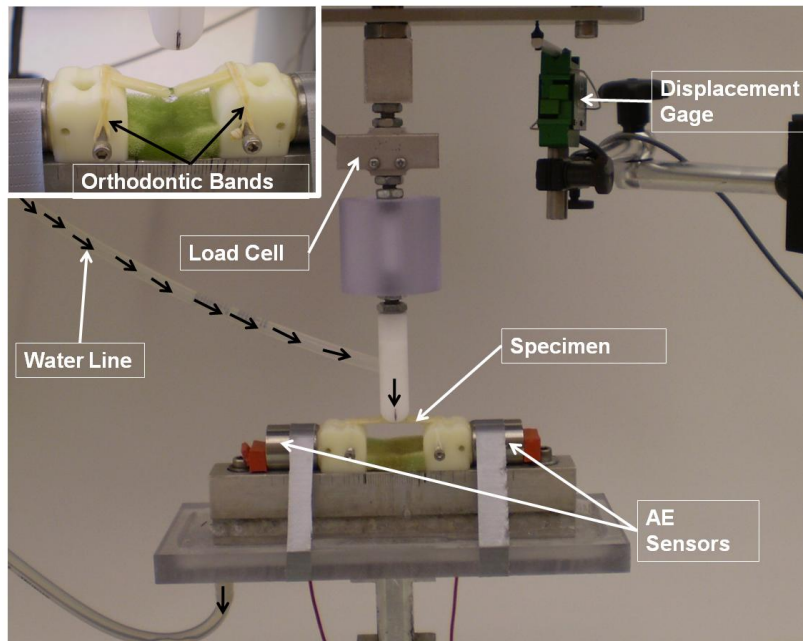


Fig. 1- Three-point bending setup: Samples were held on the bottom supports with orthodontic bands. AE sensors are located on the sides of the bottom supports. Samples were kept wet during the experiments with distilled water drips from the loading tip. A tubing was attached to the loading tip to supply the water.

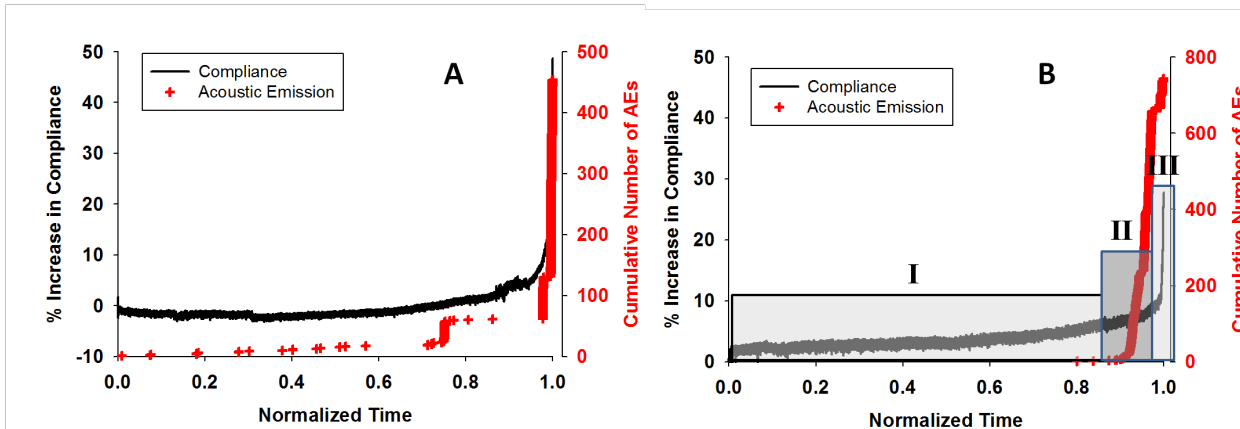


Fig. 2- Confounding AE events from aluminum supports (A) and typical Compliance vs Cumulative Number of AE graphs with Delrin supports (B): Samples tested with aluminum supports released AEs throughout the test due to rubbing on the supports (A). Since Delrin supports eliminated the rubbing, AEs were released close to failure (B).

2) *Measurement of the attenuation of acoustic emission waves in bone and other tissues,*

Ultrasound attenuation in bone and muscle analog homogenates are known in the literature. However, prior studies covered the frequency range of 500 kHz and above whereas acoustic emissions are recorded in the range 10 kHz to 500 kHz. In the current study, we focused on identifying the attenuation of acoustic emission waves in bone and muscle tissues in a frequency range which is more relevant to acoustic emissions.

The general approach of the study was such that specimens of varying thicknesses were prepared from muscles and bones. Acoustic emission waves were pulsed through these media and the reduction in waveform amplitude as a function of increasing tissue thickness was measured. The slopes of amplitude thickness plots yielded the attenuation of emissions in units of dB/cm. Attenuation was recorded for wave propagation along the transverse axis (direction transverse to longer axis of bone's shaft) and the longitudinal axis of bone. For the muscle tissue, only the transverse axis (axis perpendicular to myofibrils) was quantified.

Acoustic emissions were generated and recorded using two piezoceramic sensors (R15, Physical Acoustics Corporation, Edison NJ), preamplifiers (Physical Acoustics Corporation, Edison NJ) and a dedicated AE system (MISTRAS 2001, Physical Acoustics Corporation, Edison NJ). Each transducer was placed on opposite surfaces of the test sample using vacuum grease. The transmitting sensor was provided with a 5 μ s square pulse train per second for 30 seconds. The amplitude of the pulse was set as 100 dB. The waves traveled through the tissue and the amplitude was collected by the other R15 sensor.

Transverse bone samples were prepared from the mid-diaphyseal shaft of a fully mineralized bovine femur (24-months old) using a low-speed diamond blade saw (Isomet 1000, Buehler, Lake Bluff, IL). The cortical shell pieces were further machined in to 15 0.75"x1" rectangular slabs of varying thicknesses. The thickness of each piece was measured twice using a micrometer (SPI2000, Swiss Precision) and the average thickness was used in later calculations. The thicknesses across which the pulses traveled ranged from 1.0 to 7.3 mm. Measurements were performed within the hour following thawing of bone slabs on the bench. Longitudinal bone samples were measured from the contralateral femur of the same animal. These segments ranged 0.34 cm to 8.34 cm in length with about 0.25 cm increments.

The reduction of wave amplitude with increasing bone thickness was linear (Fig. 3). The amount of attenuation was calculated as the slope of the best fit line and expressed in terms of decibel degradation per centimeter of tissue. The data show that, on average, for every centimeter an acoustic emission travels in the transverse and longitudinal directions in bone, the amplitude will be lowered by 2.48dB and 2.52dB, respectively. Despite the material anisotropy of bone, the attenuation was comparable in longitudinal and transverse axes.

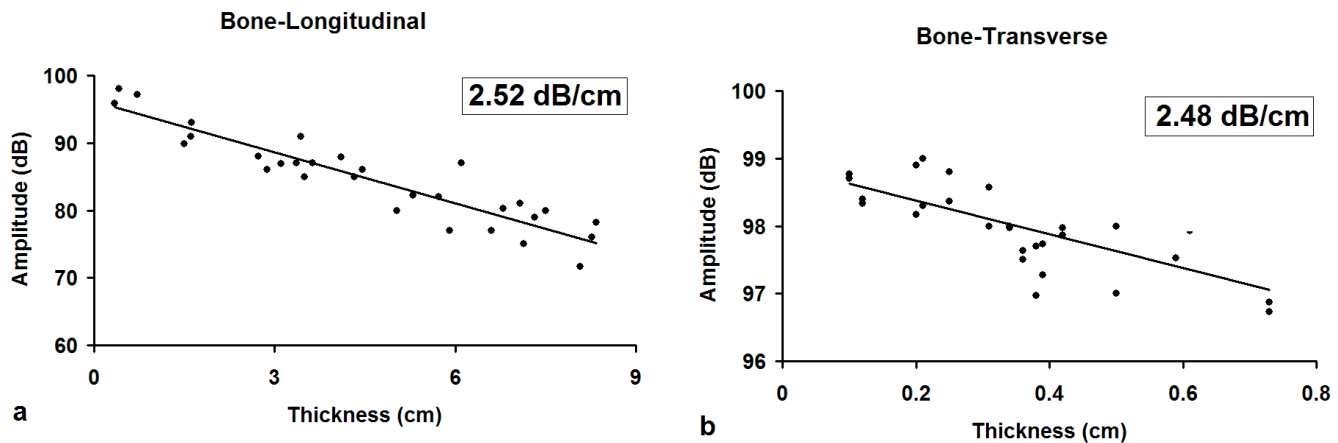


Figure 3: Attenuation of acoustic emission waves along the primary axes of bone.

3) *Measurement of acoustic emission amplitude associated with microcrack formation.*

We investigated the intensity of bone microdamage near its source via an in vitro micromechanical test model. A special specimen that included microcantilevers made from bone was used for this purpose. The microbeams were broken by a sensitive loading set up and the strength of emissions were measured right at the source (Fig. 4).

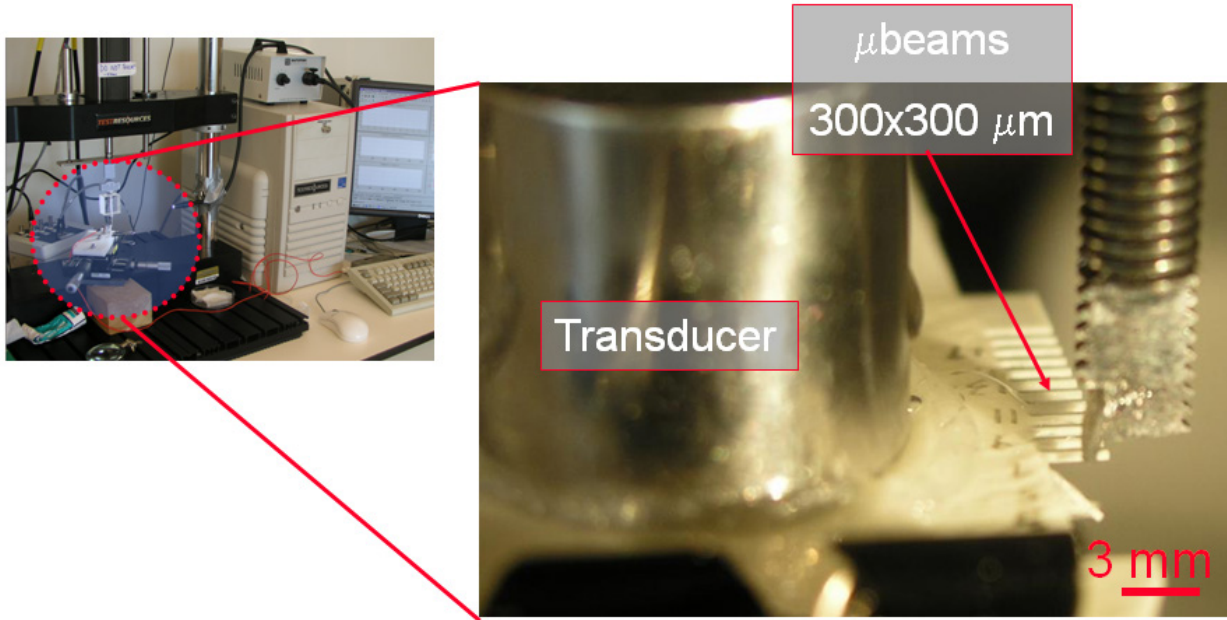


Figure 4: Microcantilever beam design for AE source strength measurement.

Specimen preparation: 15 cantilever microbeams with cross sectional dimensions of 300x300 microns were longitudinally machined out of bovine femur using a low speed saw (Buehler). These cross sectional dimensions are within the range that is reported for in-vivo microcracks. Beams were 3 mm in length and extended at the edge of bone wafers akin to a comb shaped wafer.

Mechanical tests, acoustic emission testing and data processing: Microcantilever beams were monotonically loaded to fracture at a displacement rate of 0.15mm/sec (Test Resources Inc.) by loading at their tip. The bone wafer to which microbeams cantilevered were mounted on translation stages which allowed positioning the loading tip at the same distance from the fixed end of each beam. Care was taken to have the location of the applied load be at the same distance in each beam. Acoustic emission sensor (R15, PAC) was mounted on the wafer at about a distance of about 5 mm from fixed ends of microbeams using high vacuum grease which served the dual purpose of adhering the wafer to the platform below and preventing the bone from drying. An AE transducer (Physical Acoustics Corp.) was placed on top of the wafer as close to the microbeams as possible. A clip-on strain gage extensometer was used to measure the displacement (Epsilon Tech. Corp.). Data secured from the mechanical testing system was processed to extract load at the fracture of each microbeam (MATLAB, Mathworks Inc.) and correlated with the amplitude of emissions resulting from each data from the AE system.

The intensity at the source was found to be higher than 100 dB (~ 1500mV). Also, a significant correlation ($p < 0.05$) was found out between AE intensity and fracture load (Fig. 2). Since the beam dimensions were chosen to be of comparable dimension to linear microcracks, it suggests a microcrack at its origin is notably “loud” (Figure. 5).

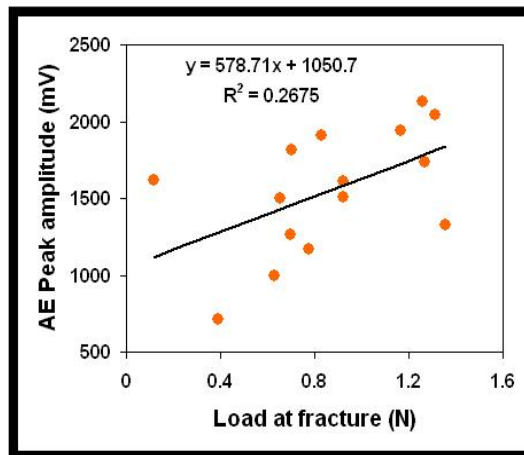


Figure 5. Peak amplitude (mV) vs. load at fracture (N).

KEY RESEARCH ACCOMPLISHMENTS

- The in vitro fatigue loading system is perfected to a degree that artifactual emissions from loading plates are eliminated. This ensures that AE waves we record are associated with failure.
- After elimination of AE waves some samples were observed to fail with very few emissions indicating that some bones are amenable to catastrophic brittle failure with no or little prior warning.
- We identified that attenuation of AE emissions in bone is at the level of 2.5 dB/cm
- We also identified that AE emissions from microcrack like specimens have more than 90 dB strength at the source.

REPORTABLE OUTCOMES

- We presented the findings of prior years at the 52nd Annual Meeting of the Orthopaedic Research Society
- Two conference abstracts are in preparation based on the results presented in this report.

CONCLUSIONS

Elimination of artifactual noise was a key aspect which now enables us to proceed with the routine fatigue tests of the remaining 30 specimens in the age range of 20 to 50 years old. In a capacity to bridge the AE method to future in vivo applications, we also determined that if microcracks were to occur in vivo, their strength at the source and the tissue attenuation as reported here will allow the transmission of waves to distances amounting to tens of centimeters. Such a propagation range indicates that waves can be detected by surface mounted sensors.